Hindawi Publishing Corporation
EURASIP Journal on Wireless Communications and Networking
Volume 2011, Article ID 749891, 18 pages
doi:10.1155/2011/749891

*Review Article*

# Comparison among Cognitive Radio Architectures for Spectrum Sensing

**Luca Bixio, Marina Ottonello, Mirco Raffetto, and Carlo S. Regazzoni (EURASIP Member)**

*Department of Biophysical and Electronic Engineering, University of Genoa, Via Opera Pia 11a, 16145 Genova, Italy*

Correspondence should be addressed to Luca Bixio, luca.bixio@dibe.unige.it

Received 28 July 2010; Revised 25 November 2010; Accepted 7 February 2011

Academic Editor: Jordi Pérez-Romero



Recently, the growing success of new wireless applications and services has led to overcrowded licensed bands, inducing the governmental regulatory agencies to consider more flexible strategies to improve the utilization of the radio spectrum. To this end, cognitive radio represents a promising technology since it allows to exploit the unused radio resources. In this context, the spectrum sensing task is one of the most challenging issues faced by a cognitive radio. It consists of an analysis of the radio environment to detect unused resources which can be exploited by cognitive radios. In this paper, three different cognitive radio architectures, namely, stand-alone single antenna, cooperative and multiple antennas, are proposed for spectrum sensing purposes. These architectures implement a relatively fast and reliable signal processing algorithm, based on a feature detection technique and support vector machines, for identifying the transmissions in a given environment. Such architectures are compared in terms of detection and classification performances for two transmission standards, IEEE 802.11a and IEEE 802.16e. A set of numerical simulations have been carried out in a challenging scenario, and the advantages and disadvantages of the proposed architectures are discussed.

## 1. Introduction

In the last decades, the introduction of new wireless applications and services is creating issues in the allocation of the available radio spectrum [1]. In fact the governmental regulatory agencies apply the *command and control* approach, which allocates different frequency bands to different transmission standards, leading to a heavily crowed radio spectrum and to a reduction of the unlicensed frequency bands [2]. However, many studies [1–3] have pointed out that licensed spectrum is highly underutilized and have encouraged to apply a more flexible and efficient management of such a precious resource to improve its utilization [1]. To this end, unlicensed (secondary) users could be allowed to access licensed spectrum if, at a given time and in a given geographical area, licensed (primary) users are not using it [1]. In particular, a proposed solution for exploiting unused resources, also known as opportunities, and for providing the required flexibility is the Cognitive Radio (CR) technology [1]. It can be defined as an intelligent wireless communication system that continuously observes the radio spectrum in order to detect opportunities which are then exploited by adaptively and dynamically selecting certain operating parameters (e.g., transmitted power, carrier frequency, modulation type and order) [1].

In such a context, it is widely accepted [4, 5] that Orthogonal Frequency Division Multiplexing (OFDM) represents one of the most appropriate approaches for CR. In fact, the OFDM technique allows to model the power spectrum of the signal, by dynamically activate/deactivate a set of carriers [5]. This property can be employed to fit the signal transmitted by secondary user to the unused spectral resources. Such a procedure can be digitally implemented by using the Discrete Fourier Transform (DFT) at the transceiver [4]. Moreover, the DFT can also be useful to detect the presence of active primary users (e.g., in the time-frequency analysis for signal detection) [4].

It is clear that, in order to efficiently utilize the radio spectrum, a fast and reliable detection of primary users is an important requirement [6]. Such fundamental task,

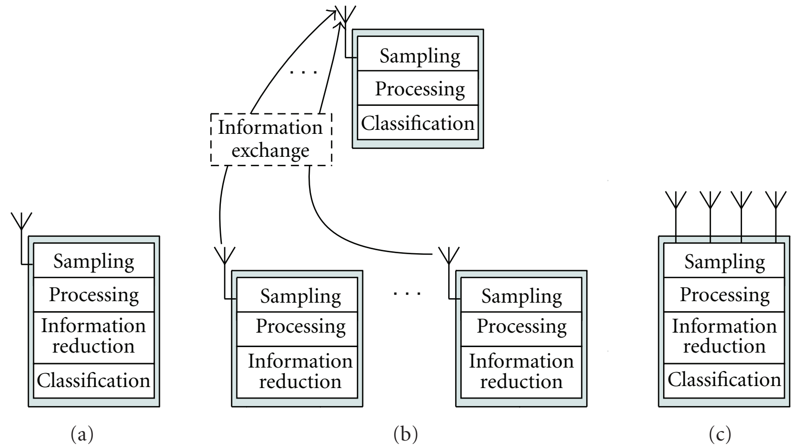


Figure 1: Considered architectures for spectrum sensing: (a) stand-alone single antenna, (b) cooperative terminals, (c) multiple antennas.

known as spectrum sensing, is performed by CR terminals which process the received signal applying advanced signal processing techniques.

Despite the fact that spectrum sensing techniques have been deeply treated in the open literature [7] for both civilian [8] and military applications [9], many open issues persist, especially in a CR scenario. As an example, many commonly employed spread spectrum transmission techniques, specifically designed to be confused with noise, are not easily identified by energy detectors [7], while matched filters cannot be easily used in a CR context [6], in which the *a priori* information about the transmitted signal is usually not available. An alternative approach to spectrum sensing is based on feature detection technique [8, 10], which allows to exploit the unique characteristics of the transmitted signals [11] in the identification of primary users. Among the proposed feature detection approaches, a recently appreciated one in CR networks is based on cyclostationary feature extraction [7, 11]. Such an approach allows to overcome the limitations of other techniques, while providing additional information regarding the frequency band under investigation [7], useful to predict the utilization of the licensed resources by the primary users [12], against an increase of the complexity of the detector. Finally, it is important to remark that such an approach is well suited to detect OFDM-based standards, since it allows to exploit the presence of periodicities in the transmitted waveform, such as cyclic prefixes or pilot carriers, as will be clarified in Section 4.

Despite the high number of spectrum sensing techniques which have been proposed in the open literature [6], and military [7] applications, spectrum sensing remains a complex task, especially in practical environments, where received signals are heavily corrupted by channel impairments (e.g., multipath fading) which can lead to an undesirable missed detection of the primary users [13, 14].

However, it is well known that multipath fading can be significantly mitigated by using several receiving antennas exploiting spatial diversity [15] since each antenna experiences an independent fading if it is approximately separated one half wavelength from each other [16–18]. To this end, different architectures can be proposed. As an example, several single antenna CR terminals can cooperate by exchanging local observations through a control channel and exploiting the spatial diversity inherent to the different positions in the considered environment. In particular, different levels of cooperation can be defined according to the amount of data exchanged among single-antenna CR terminals [19] resulting in different performances, required processing capabilities and overhead. An alternative architecture is based on a multiple antenna terminal, which exploits the spatial diversity due to the different signals perceived by the antennas. In this case, a control channel is not necessary but additional hardware costs are present.

In this paper, a relatively fast and reliable spectrum sensing algorithm for the detection of similar OFDM-based primary transmissions has been considered and applied to evaluate the performances of three different architectures. In particular, a single detector able to distinguish among three classes of signal is used. It is based on cyclostationary features extraction and exploits the periodicities in the transmitted waveforms which arise from different pilot carrier patterns and the cyclic prefix. The extracted features are then used as input to a support vector machine (SVM) which allows to identify and classify the primary users' signal. It is important to remark that the proposed work is focused on the attempt of verifying the added value derived from the introduction of the cooperation among terminals or of the multiple antenna technology to spectrum sensing. To this end, the benefits due to the introduction of the spatial diversity are investigated by analyzing the performances of the three different architectures discussed (see Figure 1) and more complex configurations will not be explored. In particular, the trade-offs among processing capabilities, the exchanged information on the control channel, and the increase of the number of terminals or antennas, with respect to the performances and the implementation costs, have been extensively evaluated.

The paper is organized as follows. In Section 2, a survey of spectrum sensing techniques and the related challenges and limitations for CR applications will be provided. In Section 3, the different architectures for spectrum sensing and the related advantages and disadvantages will be presented. Section 4 will describe the proposed spectrum sensing algorithm for the detection of two OFDM-based transmissions, its application to the spectrum sensing architectures, and a qualitative evaluation of the trade-offs will be discussed in Section 5. Finally, numerical results will be provided in Section 6 to evaluate the performances of the proposed architectures in heavy multipath environments and to quantify the benefits due to the introduction of spatial diversity.

## 2. Spectrum Sensing Techniques: Limitations and Challenges

Spectrum sensing is one of the most important tasks which a CR terminal has to perform [6] since it allows to obtain awareness regarding spectrum usage by reliably detecting the presence of primary users in a monitored area and in a given frequency band [6].

*2.1. Signal Processing for Spectrum Sensing.* In order to provide a fast and reliable spectrum sensing, different techniques have been proposed in the last decades [7–9, 20] for signal detection [7], automatic modulation classification [8], radio source localization [9], and so forth.

One of the most commonly used approach to detect the presence of transmissions is based on energy detector [20], also known as radiometer, that performs a measurement of the received energy in selected time and frequency ranges [20]. Such measurement is compared with a threshold which depends on the noise floor [6]. The presence of a signal is detected when the received energy is greater than an established threshold. Energy detector is widely used because of its low implementation, computational complexity and, in the general case where no information regarding the signal to be detected is available, is known to be the most powerful test and can be considered as optimal. On the other hand, energy detector exhibits several drawbacks [6, 10] which can limit its implementation in practical CR networks. In fact, the computation of the threshold used for signal detection is highly susceptible to unknown and varying noise level [7], resulting in poor performance in low Signal to Noise Ratio (SNR) environments [7]. Furthermore, it is not possible to distinguish among different primary users since energy detectors cannot discriminate among the sources of the received energy [14]. Finally, radiometers do not provide any additional information regarding the signal transmitted by the primary users [6, 12] (e.g., transmission standard, modulation type, bandwidth, carrier frequency) which can be useful to predict spectrum usage by primary users [12], allowing to avoid harmful interference while increasing the capacity of CR networks [10].

When the perfect knowledge of the transmitted waveform (e.g., bandwidth, modulation type and order, carrier frequency, pulse shape) [6, 14] is available, the optimum approach to signal detection in stationary Gaussian noise is based on matched filters [10]. Such a coherent detection requires relatively short observation time to achieve a given performance [6] with respect to the other techniques discussed in this section. However, it is important to note that, in CR networks, the transmitted signal and its related characteristics are usually unknown or the available knowledge is not precise. In this case, the performances of the matched filter degrade quickly, leading to an undesirable missed detection of primary users [21]. Moreover, this approach is unsuitable for CR networks, where different transmission standards can be adopted by primary users [14]. As a matter of fact, in these cases, a CR terminal would require a dedicated matched filter for each signal that is expected to be present in the considered environment, leading to prohibitive implementation costs and complexity [14].

An alternative approach to spectrum sensing is based on feature detection [7, 14, 22, 23]. Such an approach allows to extract some features from the received signals by using advanced signal processing algorithms and it exploits them for detection and classification purposes [22, 23]. In the spectrum sensing context, a feature can be defined as an inherent characteristics which is unique for each class of signals [21] to be detected. To perform signal detection, some commonly used features are instantaneous amplitude, phase, and frequency [8]. Among the different feature detection techniques which have been proposed in the open literature [7, 8, 24], an approach which has gained attention due to its satisfactory performances [7, 11, 25] is based on cyclostationary analysis, which allows to extract cyclic features [6, 7, 11, 26, 27]. Such an approach exploits the built-in periodicity [7] which modulated signals exhibit since they are usually coupled with spreading codes, cyclic prefixes, sine wave carriers, and so forth, [10]. The modulated signals are said to be cyclostationary since their mean and autocorrelation functions exhibit periodicities, which can be used as features. Such periodicities can be detected by evaluating a Spectral Correlation Function (SCF) [11, 25], also known as cyclic spectrum [7], which, furthermore, allows to extract additional information on the received signal which can be useful to improve the performance of the spectrum sensing [12]. One of the main benefits obtained by using cyclostationary analysis is that it allows an easy discrimination between noise and signals even in low SNR environments [7]. Moreover, such an approach allows to distinguish among different primary users since unique features can be extracted for the classes of signals of interest. In spite of these advantages, cyclic feature detection is computationally more complex than energy detection and can require a longer observation time than matched filters [3]. However, the proposed algorithm allows to obtain satisfactory detection performances in a relatively short observation time as will be shown in Section 6 by numerical examples.

*2.2. Signal Classification for Spectrum Sensing.* In common CR networks, the signal received by the secondary terminal is usually processed by applying one of the algorithms presented in the previous section, in order to perform signal detection [14, 28]. It allows to identify opportunities (i.e., primary unused resources) which have to be exploited by secondary user without causing harmful interference to primary users [12]. Moreover, in this paper, it is assumed that a signal classification of the detected primary signal into a given transmission standard is performed. It can be useful to improve the radio awareness [1, 12, 29] allowing to predict some spectrum occupancy patterns of the primary user, which indeed may be used to efficiently exploit the opportunity and, consequently, to increase the utilization of the resource and the throughput of the CR network [12]. Signal Classification is usually done by applying well-known pattern recognition methods to a processed sampled version of the incoming signals [30].

In general, the design of a classifier concerns different aspects such as data acquisition and preprocessing, data representation, and decision making [30]. In CR applications, data acquisition is represented by analog-to-digital conversion (ADC) of the electromagnetic signal perceived by the antenna, while the preprocessing is represented by the signal processing techniques presented in Section 2.1. The data representation could be provided by some extracted features which can be then used for decision making which usually consists in assigning an input data (also known as pattern) to one of finite number of classes [31].

Among the approaches which can be used for classification, Neural Networks (NNs) and SVMs have recently gained attention for spectrum sensing purposes [32, 33]. One of the most important advantages is that these tools can be easily applied to different classification problems and usually do not require deep domain-specific knowledge to be successfully used [30].

Recently, there has been an explosive growth of researches about NNs resulting in a wide variety of approaches [34]. Among them, the most appreciated one is feedforward NNs with supervised learning [34] which are widely used for solving classification tasks [34]. Although it has been shown that NNs are robust in the classification of noisy data, they suffer in providing general models which could result in an overfitting of the data [34].

SVMs represent a novel approach to classification originated from the statistical learning theory developed by Vapnik [35], their success is due to the benefits with respect to other similar techniques, such as an intuitive geometric interpretation and the ability to always find the global minimum [34]. One of the most important features of an SVM is the possibility to obtain a more general model with respect to classical NNs [35]. This is obtained by exploiting the Structural Risk Minimization (SRM) method which has been shown to outperform the Empirical Risk Minimization (ERM) method applied in traditional NNs [35]. SVMs use a linear separating hyperplane to design a classifier with a maximal margin. If the classes cannot be linearly separated in the input data space, a nonlinear transformation is applied to project the input data space in a higher-dimensional space, allowing to calculate the optimal linear hyperplane in the new space. Due to its widespread applications, nowadays different efficient implementations of SVM are available in the open literature [36, 37] and only few decisions regarding some parameters and the architecture have to be addressed in order to provide satisfactory performances.

Finally, some works pointed out that SVMs require a long training time, that is, the time needed to design an efficient classifier adjusting parameters and structure [34]. However, SVMs can be still applied to spectrum sensing since the design of the classifier can be done off-line exploiting some a priori measurements which can be used as training data.

*2.3. Spectrum Sensing Limitations.* Although advanced signal processing and pattern recognition techniques can ease the task of spectrum sensing, several limitations and challenges remain, especially when real environments are considered [6, 14]. In fact, CR terminals have to detect any primary user's activity within a wide region corresponding to the coverage area of the primary network and the coverage area of the CR networks [14]. For this reason, a CR terminal needs a high detection sensitivity [14] which is a challenging requirement for wireless communications, especially when spread spectrum transmission techniques are used by primary users.

Furthermore, spectrum sensing is more complex in those frequency bands where primary users can adopt different transmission standards, for example, Industrial, Scientific, and Medical (ISM) band. In this case, a CR terminal has to be able to identify the presence of primary users detecting different kinds of signals, each one characterized by its features, by using a single detector to limit hardware costs.

Finally, it is important to remark that in wireless communications the received signal is corrupted by multipath fading, shadowing, time varying effects, noise, and so forth. These phenomena can cause significant variations of the received signal strength and, thereby, it could be difficult to perform reliable spectrum sensing [13, 14]. This is of particular importance in CR networks, where a false detected opportunity, for example, due to a sudden deep fade, can lead to an incorrect spectrum utilization, causing harmful interference to primary users [13, 14].

As a final remark, in order to efficiently utilize the available radio resources, the duration and periodicity of the spectrum sensing phase have to be minimized. In fact, the opportunities have often a limited duration and CR terminals usually cannot exploit them [6, 14], while performing spectrum sensing.

## 3. Architectures for Spectrum Sensing

In this section, the main classes of spectrum sensing architectures will be shown. In particular, stand-alone single antenna, cooperative, and multiple antenna architectures will be considered (see Figure 1).

One of the most simple and widespread architectures is based on a stand-alone single antenna terminal. In this case the CR terminal, equipped with a single antenna, acts autonomously to identify the signals transmitted by the primary users on the observed frequency band [10]. The phases of the spectrum sensing process for this simple architecture are four and can be denoted as sampling, processing, information reduction, and classification, as shown in Figure 1(a). It is important to remark that, although similar architectures have been proposed in literature [22, 23], no information reduction phase is performed.

Let us analyze in detail each phase. The CR terminal exploits the single antenna to collect the signals radiated by primary transmitters. The amount of time employed for the signal collection is the so-called observation time. This quantity should be as short as possible [14] in order to maximize the exploitation of the detected opportunity [6]. The received signal is sampled and then processed: as shown in Section 2.1, different advanced signal processing algorithms can be used, according to the available knowledge of the primary signals to be identified. As an example, feature detection-based techniques can be used in order to extract the unique characteristics of the different signals which can then be used for classification purposes.

To simplify the problem, decreasing the complexity of the following classification phase and shortening the global elapsing time, the information contained in the highlighted characteristics can be reduced. As an example, classical eigenvalue method for linear feature reduction [38], used in pattern recognition, can be applied in order to reduce the problem complexity.

Once the processing and the information reduction phases are performed, and the differences among signals are pointed out, a classification phase is required to discriminate among the signals transmitted by primary users. Different techniques, presented in Section 2.2, can be used in order to obtain a precise classification phase. As an example SVM [34, 36, 37] is a well-known classifier which can be used for different problems and applications.

Despite the fact that the simplicity of the stand-alone single antenna architecture makes it attractive from an implementation point of view, it suffers in multipath and shadowing environments [16, 21] where the deep and fast fades of the received signal strength and the hidden node problem can lead to an incorrect spectrum utilization [6, 13], In order to mitigate such drawbacks, a longer observation time can allow to achieve satisfactory performances, but such a solution is not exploited in practice since fast opportunity detection is desirable in practical CR networks [6].

To overcome the disadvantages of the stand-alone single antenna architecture, cooperative and multiple antenna architectures can be proposed [6, 21]. In particular, while both cooperative and multiple antenna system can be employed to mitigate multipath fading, just cooperative approach can be used to limit shadowing effects.

Multipath (fast) fading, that is, deep and fast fades of the received signal strength, is the most characteristic propagation phenomenon in multipath environments. However, its degrading effects can be overcome by exploiting the spatial diversity due to the different positions of the CR terminals or of the several receiving antennas, in cooperative and multiple antenna systems, respectively. In fact, the antennas separated one wavelength or more are expected to obtain uncorrelated signals [17, 18] and thereby each antenna receives a signal corrupted by an independent multipath channel providing the required diversity [16], which can be exploited for improving radio awareness [2].

As opposed to fast fading, which is a short-time scale phenomenon, the so-called shadowing or slow fading, a long-time scale propagation phenomenon, can also be considered. This effect occurs when the transmitted signal experiences random variation due to blockage from objects in the signal path, giving rise to random variations of a received power at a given distance [16]. This phenomenon can cause the undesiderable hidden node problem [6, 13], that can be still overcome by means of spatial diversity. However, in this case, the receiving antennas need to be separated by much more than one wavelength since the shadowing process is frequently correlated over larger distances, in the order of some tens of meters or more. This means that the multiple antenna architecture would not be able to overcome the hidden node problem since all received signal versions would be affected by the same level of shadowing attenuation. On the contrary, the cooperative architecture may be able to overcome the hidden node problem if the cooperating CRs are apart enough to receive sufficiently uncorrelated versions of the same primary signal.

As regards the other aspects, firstly let us consider the cooperative architecture where the CR terminals form a distributed network sharing the collected information in order to improve the performances of the spectrum sensing phase [2].

Different strategies of cooperation and network topologies can be implemented: in this paper, a centralized network is considered. In particular, the proposed architecture is composed by a set of cooperative single antenna terminals, as shown in Figure 1(b), which individually sense the channel, sample and process the received signal, and finally send the collected information to a fusion center, usually represented by a predefined terminal belonging to the network with enhanced signal processing capabilities. It aggregates the received local observations [19] for identifying the signals transmitted by primary users.

Among the advantages of such an architecture, it is important to remark that it allows not only a performance improvement, as will be shown in Section 6, but also is well suited for IEEE 802.22 WRAN [3], where a base station can act as a fusion center [13]. As regards the costs, it is possible to highlight that, on one hand, the cooperative CR terminals can achieve the same performances of a stand-alone CR terminal by using less performing and cheaper hardware [13]. On the other hand, the increase of the number of terminals leads to a consequent rise in costs. Moreover, the information forwarded to the fusion center implies the introduction of a dedicated control channel (not always available in CR contexts), and a consequent coarse synchronization, to avoid a modification of the electromagnetic environment during the spectrum sensing phase.

Since a control channel may not be available in practical CR applications, a multiple antenna architecture can be considered as an alternative solution for providing the useful spatial diversity.

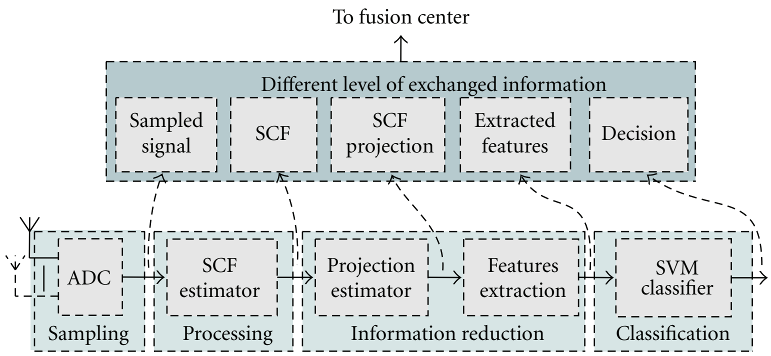


Figure 2: Block diagram for the spectrum sensing algorithms for the considered architectures.

In such an architecture, the CR terminal receiving antennas are thought as an antenna array with a digital beamforming receiving network, as shown in Figure 1(c). This strategy, that is similar to a distributed system architecture with an ideal control channel (i.e., no transmission delay and channel distortions), exploits the complexity of the environment, as happens for multiple-input multiple-output systems [16].

Multiple antenna architectures do not require a control channel and allow to take advantage from the spatial diversity [16] also for the opportunity exploitation, by managing the radiation pattern so as to mitigate the interference with primary users [39]. However, the previouse advantages are paid in terms of an increase of the hardware costs due to the presence of several receiving antennas and to the higher processing capabilities required for real-time aggregation of the signals gathered by each antenna.

Note that essentially the same processing chain, shown in Figure 1(a), can be applied to all the considered architectures. However, there are some differences. The most evident one is the introduction of an information exchange phase, if the cooperative architecture is considered.

Finally, a comprehensive analysis will be provided in the following, by comparing the performances and implementation trade-offs pointed out in this section, for the standalone single antenna, the cooperative single antenna, and the multiple antenna architectures.

## 4. Reference Scenario and Proposed Analysis

In the present section, the developed algorithms to perform a reliable spectrum sensing phase in CR networks are deeply analyzed. They can be grouped in the processing chain shown in Figure 2, composed by four main phases, that is, sampling, processing, information reduction, and classification. Each phase is detailed in the following.

In order to provide a fair comparison of the performances obtained by the three architectures, they implement the same logical scheme shown in Figure 2 (with a few exceptions related to the introduction of the information exchange phase). Moreover, the same signal processing algorithm for each phase of the chain is applied and, for the same reason, only multipath fading is considered in the simulations.

Note that the considered processing algorithms, proposed as full proof in [33], have been exploited in other works [21, 40–42]. However, the performances of these algorithms have not been extensively evaluated yet. In fact, in [41] the influence of the dimension of an ensemble of neural networks in the classification phase is studied, while in [40] the analysis is focused on a comparison of different data fusion techniques for cooperative spectrum sensing. Moreover, although in [21, 42] an analysis of the proposed algorithms is presented, only a few results and discussions related to the performances have been reported for a cooperative architecture [42] and for a multiple antenna architecture [21].

In this paper, we are interested in comparing the performances of the considered algorithms when applied to the three architectures of interest. In particular, a deep comparative analysis of the performances of the three architectures will be presented, evaluating the relations among processing capabilities (and hence the information reduction), the exchanged information on the control channel, and the increase of the number of terminals or antennas, with respect to the performances and the implementation costs. To this end a comprehensive qualitative and quantitative analysis will be provided in the following sections.

As a final remark, in [21, 33, 40–42], the CR receiver is supposed to be synchronized in the time domain with the primary transmitter (i.e., the input of the processing phase is represented by a set of entire number of OFDM symbols) which is an undesirable hypothesis in practical scenarios. Differently, in this paper, no synchronization assumption is assumed to obtain the experimental results provided in Section 6. For this reason, the proposed algorithm can be considered semiblind since the only parameters needed to perform the detection are the bandwidth and the number of samples in an OFDM symbols. The estimation of this parameters is out of scope of the present paper; however, they can be obtained by applying some algorithms presented in the open literature [43].

The performance of the three architectures is evaluated in a challenging scenario, in which one CR terminal (single or multiple antenna) or several CR terminals (cooperative) have not only to detect the presence of a primary user, but also to classify the used transmission standard. It is important to remark that, in order to provide an upper bound for the achievable performances, just one primary user is considered in the frequency band of interest, as usually considered in the literature [2, 5, 11, 12].

The primary user can transmit IEEE 802.16e [44] or IEEE 802.11a [45] signals in the same frequency band. Such signals are very similar, since both the considered standards use the same transmission technique (i.e., OFDM), and are intentionally designed to occupy the same bandwidth, as will be explained in Section 4. Moreover, the signal transmitted by the primary user is corrupted by Additive White Gaussian Noise (AWGN) and heavy multipath distortions [46], that can lead to an undesirable missed detection.

Finally, in order to summarize the analyzed configurations, let us indicate $CA_n^t$ as a CR architecture in which the subscript $n \in \{1, 3, 5, 7\}$ denotes the number of cognitive terminals that compose the system, while the superscript $t \in \{1, 3, 5, 7\}$ denotes the number of antennas that equip each terminal. By using the introduced notation, let us analyze in details the different architectures:

(1) $CA_1^1$ for the stand-alone single antenna architecture,

(2) $CA_n^1$ with $n = 3, 5, 7$ for the cooperative architecture. In this case, a control channel is introduced and one of the CR terminals belonging to the centralized network acts as fusion center,

(3) $CA_1^t$ with $t = 3, 5, 7$ for the multiple antenna architecture. Each antenna receives a different signal, that is sampled and put besides to the other ones to form a longer signal that is then processed.

*4.1. Sampling and Processing Phases.* Let us analyze in detail the spectrum sensing algorithms which equip the three considered architectures.

At first, during the sampling phase, each antenna senses the radio environment and raw data are collected by sampling the received signal.

In the next phase that is, the processing phase, the sampled signal is analyzed by using a cyclostationary analysis. It is important to note that if the multiple antenna architecture is considered, the sampled signal received by each antenna is placed side by side to form a longer signal which is then processed. As pointed out in Section 2, cyclostationary analysis allows to extract valuable information regarding the correlation of the spectral components of the signals under investigation, overcoming the difficulties of low SNR environments. It is well suited to the proposed architectures since it allows to exploit the periodicities that arise in the modulation process of the OFDM signals, such as cyclic prefixes, pilot carriers, or training symbols. In particular, an evaluation of the SCF is provided by using the following discrete time estimator [11]:

$$S_x^{\alpha}(k) = \frac{1}{L}\sum_{l=1}^{L} X_l(k) X_l^*(k-\alpha) W(k), \tag{1}$$

where $W(k)$ is a spectral smoothing window [11]. $\alpha$ is the discrete cyclic frequency which represents the distance, in the frequency domain, among the spectral components of the sampled signal $x(n)$, processed in $L$ blocks of length $N_{\mathrm{SCF}}$, while $X_l(k)$ represents the DFT of $x(n)$ of size $N_{\mathrm{SCF}}$:

$$X_l(k) = \sum_{n=0}^{N_{\mathrm{SCF}}-1} x(n) e^{-j(2\pi/N_{\mathrm{SCF}})kn}. \tag{2}$$

The SCF is hence obtained by processing $L \cdot N_{\mathrm{SCF}}$ samples of the received signal. It is of interest to recall that the SCF reduces to the conventional power spectral density function for $\alpha = 0$ while, in general, it represents a measure of the correlation between the spectral components of the signal $x(n)$ at the discrete frequencies $k$ and $k - \alpha$ [7].

Although the SCF is a powerful tool, it has to be properly designed in order to extract valuable periodicities. As a matter of fact, if the sampling frequency does not correspond to an integer multiple $\beta$, also known as oversampling factor, of the one used by the OFDM transmitter, or if the $N_{\mathrm{SCF}}$ parameter is not set equal to the size of the DFT used by the transmitter, then the SCF does not exhibit periodic behavior and reliable spectrum sensing cannot be obtained [33]. For the above reasons, an ad hoc SCF estimator has to be designed for each class of primary users' signals to be classified. Such a necessity can lead to an undesirable increment of hardware costs, since for each transmission standard a properly designed SCF estimator is required.

One of the features of the considered approach is to reduce the required computational effort, by equipping the CR terminals with a single SCF estimator, based on (1) and designed for classifying the three classes of signal of interest: IEEE 802.16e [44], IEEE 802.11a [45], and no transmission (in this case, only noise is received). Note that, although the required computational effort is considerably decreased, the proposed single SCF estimator leads to a satisfactory performance, as will be shown in Section 6, since just a negligible decrement of the performances is obtained in classifying IEEE 802.16e signals. Such approach exploits the periodicities that arise from the pilot carriers, commonly used in OFDM systems for channel estimation and synchronization purposes, in order to distinguish among the considered classes of signals. As a matter of fact, the time-frequency patterns of the pilot carriers, intentionally embedded in the waveform transmitted by using both considered transmission standards, are different. This leads to different periodicities, which can be detected if the SCF estimator is correctly designed. In order to obtain the required single SCF estimator, the parameters in (1) are set so that the periodicities regarding IEEE 802.11a [45] signals can be easily extracted, while distorted but still clear features for IEEE 802.16e [44] signals can be obtained, as will be described in Section 4.2.

As can be easily noted in Figure 3, the SCF for an IEEE 802.11a [45] signal exhibits a periodic behavior due to the correlation among the pilot carriers, which can be used as features in order to detect primary user's transmission. It is important to remark that Figure 3 is obtained by processing a signal of $L = 500$ blocks and with an energy per bit to noise power spectral density ratio of $E_b/N_0 = 0$ dB. Hence, clear features can be pointed out by using the SCF estimator even in low SNR environment and with short observation times.

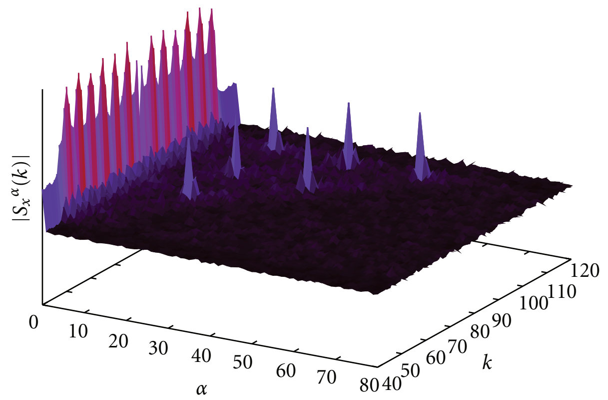


Figure 3: SCF estimation for an IEEE 802.11a signal with $L = 500$ and $E_b/N_0 = 0$ dB.

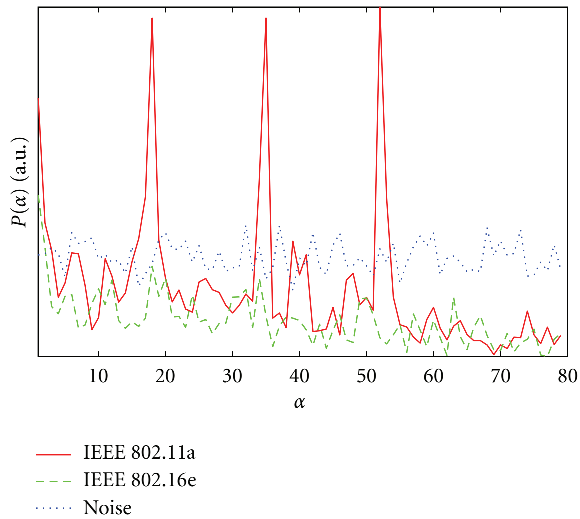


Figure 4: Projection $P(\alpha)$ for an IEEE 802.11a signal, an IEEE 802.16e signal, and no transmission (noise) with $L = 500$ and $E_b/N_0 = 0$ dB.

*4.2. Information Reduction Phase.* In order to reduce the amount of data to be processed during the classification phase, that can heavily affect the elapsing time, the information reduction is performed after the SCF processing, as shown in Figure 2.

In the proposed approach, the first information reduction step allows to compress the whole amount of data of the three-dimensional SCF by evaluating its normalized projection:

$$P(\alpha) = \frac{\max_k |S_x^{\alpha}(k)|}{\max_k |S_x^{0}(k)|}, \quad \alpha = 1, \ldots, \frac{N_{\mathrm{SCF}}}{\beta}. \tag{3}$$

Figure (4) shows the projections $P(\alpha)$ for an IEEE 802.11a signal, an IEEE 802.16e signal, and noise with $L = 500$ and $E_b/N_0 = 0$ dB. One can deduce that, although the amount of data has been significantly reduced, the periodicity is still clearly visible and it is represented by the peaks in the projection.

The second reduction step for further compressing the information can be performed by extracting two features from the projection for each class of signals of interest. In particular, this is done by using

$$F_{\Gamma_i} = \frac{\sum_{\alpha \in \Gamma_i} P(\alpha)}{\sum_{\alpha \notin \Gamma_i} P(\alpha)}, \quad i = 1, 2, \tag{4}$$

where $\Gamma_i$ is a set of values of $\alpha$ which points out the periodic behavior (i.e., the unique characteristic) of the considered signals.

To this end, the set $\Gamma_1$ allows to discriminate between IEEE 802.11a [45] and IEEE 802.16e [44] signals exploiting the second-order cyclostationarity arising from the pilot carrier insertion. In particular, IEEE 802.11a [45] pilot carriers are equally spaced in the frequency domain of an integer number of carrier spacing (i.e., the inverse of the OFDM symbol duration [16]) leading to a peak in the SCF at a given cyclic frequency (see Figure 4) given by

$$\left\{\alpha_j \in \Gamma_1\right\} = \left\lfloor \frac{N_{\mathrm{SCF}}}{\beta} \frac{j}{N_{\mathrm{FFT}}} d \right\rfloor, \quad j = 1, \ldots, J-1, \tag{5}$$

where $d$ is the distance in carrier spacing among the equally spaced pilot carrier, $N_{\mathrm{FFT}}$ is the DFT size at the IEEE 802.11a [45] transceiver, and $J$ is the number of pilot subcarrier. The set $\Gamma_2$ allows to discriminate among noise and OFDM-based transmissions, exploiting the second-order cyclostationarity arising from the presence of the cyclic prefix [16] in both IEEE 802.11a [45] and IEEE 802.16e [44] transmission standards [11]. Such a cyclostationarity leads to a higher value of the SCF of the OFDM-based transmissions for the first cyclic frequencies [11] with respect to the one of the noise (see Figure 4). In this work, the most significant cyclic frequency (i.e., the one which leads to the highest value in the SCF) has been considered

$$\{\alpha \in \Gamma_2\} = \left\lfloor \frac{N_{\mathrm{SCF}}}{\beta} \frac{1}{N_{\mathrm{FFT}}} \right\rfloor. \tag{6}$$

In this work, $N_{\mathrm{SCF}} = 160$, $\beta = 2$, $N_{\mathrm{FFT}} = 64$, $J = 4$, and $d = 14$ have been chosen. By applying these values in (5) and in (6), one can obtain the sets $\Gamma_1$ and $\Gamma_1$ as follows:

$$\begin{aligned} \Gamma_1 &= \{17, 35, 52\}, \\ \Gamma_2 &= \{1\}. \end{aligned} \tag{7}$$

An example of the features extracted by using (4) is shown in Figure 5. In particular, it represents the features for the three classes of signal of interest for $E_b/N_0 = 0$ dB and $L = 500$ processed blocks (i.e., an observation time of 2 (ms)). Note that, although the received power and the observation time are relatively low, the features representing each class are fairly clustered and can be easily identified. Such a property is exploited in the following phase for classifying the primary signal.

It is important to remark that the information reduction step allows the three proposed architectures to shorten the classification time, and hence the entire computation time. This is of fundamental importance in CR application since any opportunity detection and exploitation have to be performed in real time. Furthermore, it allows to reduce the amount of information exchanged on the control channel, when the cooperative architecture is used.

In particular, different amount of data can be sent by the CR terminals to the fusion center or can be used as input to the classification phase of the stand-alone single antenna and multiple antenna architectures. Let us analyze in detail such aspect by considering the different amount of information which can be managed in the presented spectrum sensing chain, that is,

(i) *the sampled signal*. In this case, the signal perceived by the antenna is sampled and directly sent to the fusion center: the CR terminal merely acts as data collectors. The signal length depends on the sampling frequency and on the observation time. As an example, for a signal observed for 2 ms and sampled at a frequency of 40 MHz, the signal length is equal to 80000 samples. Such a configuration requires high channel and computational capabilities, respectively, to send and to process the entire collected signals at the fusion center, a tough problem in real environments,

(ii) *the SCF*. In this case, the received signal is sent to the fusion center after the sampling and the SCF processing by using (1). The length of the three-dimensional SCF is equal to $(N_{\mathrm{SCF}}/\beta)^2$ samples. Usually $N_{\mathrm{SCF}}$ is a high number (e.g., 128, 256), and even in this case, the amount of exchanged information can be unsuitable in a practical CR scenario,

(iii) *the SCF profile*. A more efficient and practical information exchange can be obtained by adding the information reduction phase to the previous considered steps by using (3). In such a way, a significant compression of the information sent on the control channel is obtained: the length of the SCF profile is only $N_{\mathrm{SCF}}/\beta - 1$ samples,

(iv) *the extracted feature*. A further improvement in the efficiency of the information exchange phase can be obtained by applying the second information reduction step by using (4). In this case, only two features (a few bits) are transmitted to the data fusion center, obtaining a framework exploitable in a real scenario,

(v) *only decision*. In such case, the CR terminals perform all the steps of the processing chain, from the sampling to the classification phase, and they transmit to the fusion center only the classification results. Although such an approach allows to further compress the information to be sent, it requires to implement a classifier at each terminal.

Since we consider a CR application where information exchange among cooperative CR terminals has to be limited, in the present contribution the extracted features, by using (4), are sent to the fusion center which exploits them for classification purposes. Moreover, in order to provide a fair comparison among the three architectures, the extracted features are used as input to the classification phase even for the stand-alone single antenna and the multiple antenna architectures.

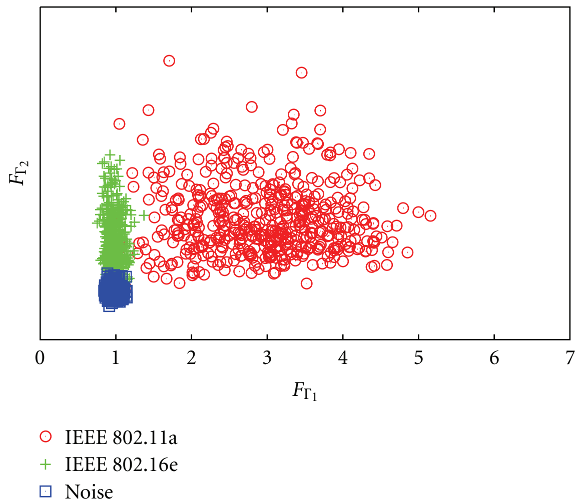


Figure 5: Plane of the features for an IEEE 802.11a signal, an IEEE 802.16e signal and no transmission (noise) with $L = 500$ and $E_b/N_0 = 0$ dB.

*4.3. Classification Phase.* During the classification phase, which represents the last step of the spectrum sensing chain (see Figure 2), the collected and processed information has to be exploited in order to detect the presence of primary users and to classify their related transmission standards.

To this end, a multiclass SVM classifier is designed. As highlighted in Section 2.2, it is a widespread approach applied to both regression and classification problems because of its satisfying performances. The basic aspects necessary for understanding the classification step are introduced in the following.

In general, the classification involves two phases known as training and testing [37]. During the training phase, some data instances composed by extracted features and class labels are used to design a classifier adjusting its parameters and structure [37]. The obtained classifier is then used during the testing phase to associate a data instance composed by extracted features to a class label [37].

In the considered scenario, a multiclass SVM classifier is needed since three possible classes are available. The "one-against-one" approach [36] is used to design the multiclass SVM composed by three binary classifier constructed by training data from the $i$th and the $j$th classes by solving the following two-class classification [36, 37]:

$$\begin{aligned}
&\min_{\mathbf{w}^{ij},b^{ij},\xi^{ij}} && \frac{1}{2}\left(\mathbf{w}^{ij}\right)^T\mathbf{w}^{ij} + C\sum_t \xi_t^{ij}\\
&\text{subject to} && \left(\mathbf{w}^{ij}\right)^T\phi(\mathbf{x}_t) + b^{ij} \geq 1 - \xi_t^{ij}, \quad \mathbf{x}_t \in i\text{th class}\\
& && \left(\mathbf{w}^{ij}\right)^T\phi(\mathbf{x}_t) + b^{ij} \leq -1 + \xi_t^{ij}, \quad \mathbf{x}_t \in j\text{th class}\\
& && \xi_t^{ij} \geq 0, \quad C > 0,
\end{aligned} \tag{8}$$

where $\mathbf{x}_t$ is the training set composed by a subset of the extracted features by using (4), $\mathbf{w}$ is the vector normal to the hyperplane, $b$ is a bias term, $\xi$ is a slack variable, $\phi(\cdot)$ is a mapping function, and $C$ is the penalty parameter of the error term. From a geometric point of view, the training vector $\mathbf{x}_t$ is nonlinearly mapped into a higher-dimensional space by using the mapping function $\phi(\cdot)$. In this higher-dimensional space, the SVM finds the optimal linear separating hyperplane [36, 37]. It is important to note that $K(\mathbf{x}_t^p, \mathbf{x}_t^q) \equiv \phi(\mathbf{x}_t^p)^T \phi(\mathbf{x}_t^q)$ is known as kernel function and it plays a key role in the nonlinear transformation. Among the different kernel functions which can be used, in this work, a radial basis function (RBF) is applied:

$$K\left(\mathbf{x}_t^p, \mathbf{x}_t^q\right) = e^{-\gamma \|\mathbf{x}_t^p - \mathbf{x}_t^q\|^2}, \quad \gamma > 0. \tag{9}$$

This function allows to manage nonlinear problems and it has already been successfully used in similar classification problems [47]. Moreover, it is less complex with respect to other functions while guaranteeing satisfying performances [36, 37]. To obtain the best multiclass SVM, the involved parameters $\gamma$ (see (9)) and $C$ (see (8)) are optimized by using a cross-validation via parallel grid-search algorithm, as proposed in [36], which guarantees the best possible performances in terms of correct detection and classification of the transmitted signals. Finally, the slack variable $\xi$ is set to the default value 0.001 which is suitable for most of the common cases and it allows to find the bias term $b$ which satisfies (8) given $C$, $\gamma$, and $\xi$ [36, 37].

## 5. An Analysis of the Performance Trade-Offs for the Three Architectures

For the three proposed systems, different considerations regarding the architectural limitations and the parameters which have to be taken into account to design efficient terminals can be pointed out. In particular, such parameters are

(i) performances,
(ii) costs,
(iii) number of antennas,
(iv) number of terminals,
(v) processing capabilities,
(vi) information reduction,
(vii) information exchange,
(viii) spatial displacement.

The evaluation problem can be simplified by splitting the variables of interest for the cooperative and multiantenna architectures as follows:

(i) for $CA_n^1$ the reduction of the information and hence its exchange through the control channel, the distribution of the processing capabilities between the data fusion center and the other terminals, and the number of terminals have to be considered in the analysis of the performances and costs;

(ii) for $CA_1^t$ the performances and the costs will be analyzed by varying the number of the antennas.

As a general remark, during the design of a cooperative or a multiantenna system, it is important to sufficiently separate the antennas (of one or more terminals) in order to take advantage of the spatial diversity, receiving uncorrelated signals. As recalled in Section 3, one wavelength is sufficient for mitigating multipath fading effects while tens of meters are required to avoid shadowing. In this sense, a low number of uncorrelated users would be more effective in overcoming the hidden node problem than a large number of correlated users, as it has been shown in many cooperative spectrum sensing studies. Since, in order to provide a fair comparison, the quantitative evaluation provided in the next section takes into account only the first effect, in the following the uncorrelation of the signals at the antennas has been always assumed. Let us provide a qualitative evaluation of the influence of the other parameters pointed out in the previous list, on cooperative and multiple antenna architectures, with respect to the stand-alone single antenna terminal.

In the cooperative architecture, an increase of the number of terminals allows an obvious improvement in the performances, but a consequent rise in cost. As regards the processing capabilities necessary to perform the spectrum sensing phase, it can be useful to point out that $P_{\text{tot}}$ that is, the total amount of processing capabilities of each architecture can be separated in $P_{\text{fusion}}$ (the processing capabilities of the data fusion center) and $P_{\text{terminal}}$ (the processing capabilities of the other cooperative CR terminals). Hence, it is possible to write

$$P_{\text{tot}} = P_{\text{fusion}} + (n-1) \cdot P_{\text{terminal}}, \quad n > 0. \tag{10}$$

Formula (10) can represent not only the cooperative architecture, but also the other ones since for $CA_1^t$ it reduces to $P_{\text{tot}} = P_{\text{fusion}}$. In fact, in such case, the signal processing algorithm is implemented in the only terminal available.

From (10), one can easily see that in the cooperative architecture, for a fixed $P_{\text{tot}}$, it is possible to reduce $P_{\text{fusion}}$ with an increase of $P_{\text{terminal}}$, or *vice versa*: that is, the tasks of the data fusion center can be simplified if the processing capabilities of the terminals increase, or *vice versa*, As an example, if each terminal performs sampling, SCF processing, information reduction, and classification, then the fusion center's tasks are reduced to simply collect the decision of the CR terminals. On the contrary, if the CR terminals perform only the sampling of the signals, all the other functions are delegated to the data fusion center: in such a case the cooperative architecture is similar to a multiple antenna one, since the CR terminals act as simple sensors, while the "intelligence" of the system resides in the data fusion center.

In this way, the distribution of the processing capabilities affects the costs: in fact, terminals will be more or less expensive in accordance with the hardware equipment needed to perform the processing.

Moreover, the distribution of the processing capabilities is strictly tied to the amount information that needs to be exchanged through the control channel. By considering the previous example, in fact, it is possible to notice that, if the CR terminals perform only the sampling of the received signals, with a consequent decrease of the hardware costs, a high channel capacity is required in order to send the entire signals to the fusion center. The amount of the exchanged information is evidently affected by $n$: an increase of the number of cooperative terminals directly corresponds to an increase of the information exchanged on the control channel.

As far as the multiple antenna architecture is concerned, the costs will increase by increasing $t$: this fact is not only due to the obvious rise in costs of the antennas, but also to a required increase of the processing capabilities. In particular, in order to obtain the same whole elapsing time of a stand-alone single antenna architecture, the multiple antenna terminal has to be equipped with higher hardware capabilities (hence more expensive). In fact, the SCF evaluation (see Figure 2) for the multiple antenna system has to be done on the signal obtained by joining the signal received by all antennas, which is $t$ times longer than the one employed by the single antenna system, if the same observation time is considered.

## 6. Numerical Results and Simulations

In order to evaluate the effectiveness of the proposed architectures, a set of simulations have been carried out. The tests have been divided into three subsections, describing the general spectrum sensing performances, the influence of the information reduction phase on the performances, and some consideration regarding the elapsed time for processing and classification phases. In particular, in the considered reference scenario, the primary users can communicate by using IEEE 802.11a [45] and IEEE 802.16e [44] transmission standards. The proposed stand-alone single antenna, cooperative single antenna and multiple antenna architectures have to detect the presence of primary users in the radio environment and to identify the related transmission standard in order to exploit the available resources. It is assumed that the antennas are sufficiently separated to each other to receive uncorrelated signals (i.e., the antenna separation is one half wavelength or more [16–18]) for both cooperative single antenna and multiple antenna architectures. In order to provide a fair comparison, shadowing effects have not been considered in the analysis. Moreover, because of the short observation times considered during the spectrum sensing phase, long-time scale propagation phenomenon can be considered constant. Under the hypothesis of the sufficient separation of the antennas, spatial diversity can be exploited and, as expected [3, 6, 10, 13, 14], an increment of the performances has been verified. It is important to recall that spectrum sensing in the proposed scenario is challenging, since both considered transmission standards adopt the OFDM technique. Moreover, the bandwidth of the IEEE 802.16e [44] transmitted signal is chosen to be equal to 20 MHz, which corresponds to the one of the IEEE 802.11a [45] transmitted signal. The modulation used on each subcarrier is Quadrature Phase Shift Keying (QPSK) for both transmission standards. Since, in this work, the performances of the proposed architectures have to be evaluated for practical applications, the received signals are affected by AWGN and heavy multipath distortions by using the COST 207—Bad Urban channel model [46] whose main characteristics are reported in Table 1 [46]. Furthermore, a Doppler frequency of $f_d = 100\,\text{Hz}$ has been considered to simulate moving users in the domain of interest.

Table 1: COST 207—Bad Urban channel model [46] parameters.

| Path number | Propagation delay ($\mu$s) | Path power (dB) | Delay spread ($\mu$s) |
|---|---|---|---|
| 0 | 0.0 | −3 | |
| 1 | 0.4 | 0 | |
| 2 | 1.0 | −3 | 2.4 |
| 3 | 1.6 | −5 | |
| 4 | 5.0 | −2 | |
| 5 | 6.6 | −4 | |

As it has been already pointed out in Section 4, a single SCF estimator has been designed to reduce hardware cost and the computational complexity. In particular, the considered processing chain is designed to easily detect IEEE 802.11a signals [45] by evaluating clear features, while IEEE 802.16e signals [44] are detected by exploiting distorted features. In fact, two important parameters which affect the effectiveness of the proposed processing chain are the sampling frequency $f_s$ and the dimension of the SCF estimator $N_{\text{SCF}}$, as shown in Section 4.1. During the performed simulations all signals are treated by using their equivalent baseband representations. We consider an $f_s = 40\,\text{MHz}$, which corresponds to an oversampling factor of $\beta = 2$. Since the proposed SCF estimator is tailored for IEEE 802.11a [45] signal detection, $N_{\text{SCF}}$ is set to 160 in order to accommodate an entire IEEE 802.11a [45] OFDM symbol. It is important to note that the proposed algorithm can be considered semi-blind since the only parameters needed to perform the detection are the bandwidth and the number of samples in an OFDM symbols. The estimation of this parameters is out of scope of the present paper; however, they can be obtained by applying some algorithms presented in the open literature [43]. In order to provide a comprehensive analysis, a wide set of simulations have been carried out to evaluate the performances of the proposed spectrum sensing phase implemented by the considered architectures, under different constraints. In particular, 500 sets of features have been generated by using

$$\Upsilon = \left\{F^{n}_{\Gamma_i}\right\}, \quad i = 1,2, \; n = 1,3,5,7 \tag{11}$$

for different values of the observation time $T_{\text{obs}} \in \{2,3,5,10\}$ (ms), energy per bit to noise power spectral density ratio $E_b/N_0 \in \{-5,0,5,10,15\}$ (dB), class of signal $S \in \{\text{IEEE802.16e}, \text{IEEE802.11a}, \text{noise}\}$, and number of cooperative CR terminals $n \in \{1,3,5,7\}$ or number of receiving antenna $t \in \{1,3,5,7\}$. Therefore, $\Omega_{\text{tot}} = 30000$ sets of features $\Upsilon$ have been generated for each number $n$ of cooperative CR terminals or for each number $t$ of receiving antenna. It is important to note that the dimension of the

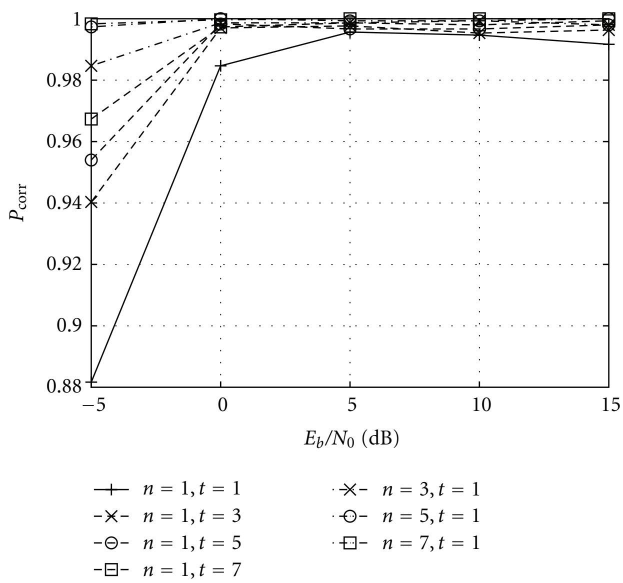


Figure 6: Probability of correct detection $P_{corr}$ versus energy per bit to noise power spectral density ratio $E_b/N_0$ for different numbers $n$ of cooperative single antenna CR terminals and multiple antenna CR terminal with a variable number $t$ of antennas.

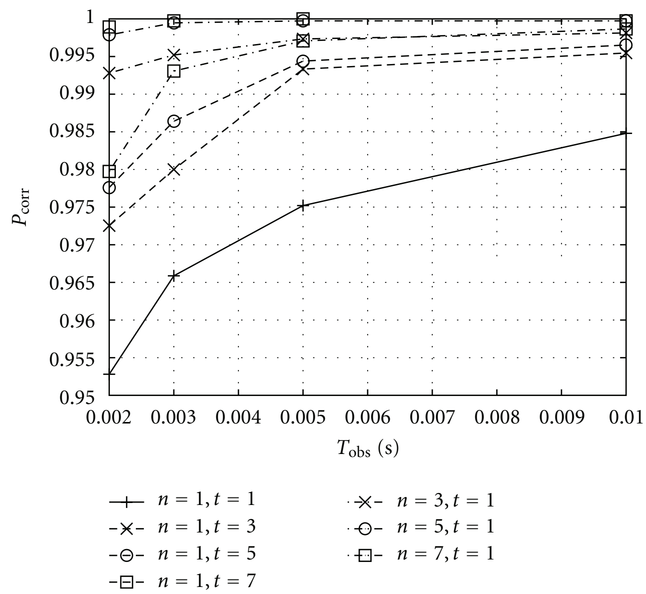


Figure 7: Probability of correct detection $P_{corr}$ versus observation time $T_{obs}$ for different numbers $n$ of cooperative single antenna CR terminals and multiple antenna CR terminal with a variable number $t$ of antennas.

set of features $\Upsilon$ depends on the number of CR terminals in the architectures. In particular, if the cooperative architecture is considered, then the dimension of $\Upsilon$ is equal to $i \times n$, where $i$ represents the number of extracted features (equal to 2 in the proposed algorithm), while if the multiple antenna architecture is considered, then the dimension of $\Upsilon$ is equal to $i$. This is due to the fact that, if a cooperative architecture is considered, the set of features sent by each terminal to the fusion center are collected by using (11). On the other hand, if a multiple antenna architecture is considered, the signals perceived by each antenna are placed side by side resulting in a longer aggregated signal to be processed. The dimension of $\Upsilon$ is important since it affects the elapsed time of the classification phase as will be clarified in the following by showing numerical examples (see Table 5(a)).

A single multiclass SVM classifier has been generated, as described in Section 4.3, for each number of cooperative CR terminals or for each number of receiving antenna by using $\Omega_{train} = 15000$ sets of features for the training phase. The set $\Omega_{train}$ is composed by an equal number of sets of features for each $E_B/N_0$, $T_{obs}$ and class of signals, in order to obtain a general classifier. Finally, $\Omega_{test} = \Omega_{tot} - \Omega_{train} = 15000$ sets of features are used for testing the obtained classifiers in order to evaluate the performances of the proposed spectrum sensing algorithms for the considered architectures.

*6.1. Spectrum Sensing Performances.* As a first example of the obtained results, in Figure 6 the probability of correct detection $P_{corr}$, that is the probability to correctly detect and classify the transmission standard used by the primary user, is reported for different values of the simulated $E_b/N_0$. Note that all the considered values of the observation time $T_{obs}$ are used to draw Figure 6. Figure 7 shows the probability of correct detection versus the considered values of $T_{obs}$. Even in this case all the considered values of $E_b/N_0$ are used to draw Figure 7. As it can be easily deduced, the performances increase as the observation time and the SNR increase, as expected. In fact, $P_{corr}$ approaches to one if high values of $E_b/N_0$ and $T_{obs}$ are considered. Moreover, the performances increase with the number $n$ of the cooperative single antenna CR terminals and the number $t$ of antennas in the multiple antenna architecture at the cost of an increment in computational complexity due to either overhead for dedicated control channel allocation and hardware cost for several receiving antennas, respectively (see Section 4.1). It is important to remark that the performances of the cooperative architecture outperform the multiple antenna architecture. This is due to the fact that, in this paper, the signals perceived by all antennas of the multiple antenna architecture are joined together with no additional elaboration, as described in Section 4. Thus, the performances reported in the figures can be considered as a lower bound for such an architecture. By applying advanced signal processing algorithms, specifically designed to combine signal exploiting diversity [16], a further improvement of the performances can be obtained. Note that, the performance reported in the figures for the cooperative architecture can be considered as an upper bound for the performances of such an architecture. In fact, an ideal control channel is supposed. In practice, in real environment, the exchanged information is corrupted by channel impairments which can negatively affect the performances. However, if the amount of data to be shared is limited, as in this case where only two

Table 2: Confusion matrices for $T_{obs} = 2$ ms.

(a) $n = 1, t = 1$

| | Noise | IEEE 802.16e | IEEE 802.11a |
|---|---|---|---|
| Noise | 98.9% | 1.1% | 0% |
| IEEE 802.16e | 9.0% | 90.2% | 0.8% |
| IEEE 802.11a | 1.4% | 1.9% | 96.7% |

(b) $n = 1, t = 3$

| | Noise | IEEE 802.16e | IEEE 802.11a |
|---|---|---|---|
| Noise | 99.3% | 0.7% | 0% |
| IEEE 802.16e | 5.5% | 94.4% | 0.1% |
| IEEE 802.11a | 0.1% | 1.8% | 98.1% |

(c) $n = 3, t = 1$

| | Noise | IEEE 802.16e | IEEE 802.11a |
|---|---|---|---|
| Noise | 99.6% | 0.4% | 0% |
| IEEE 802.16e | 1.7% | 98.3% | 0% |
| IEEE 802.11a | 0% | 0.1% | 99.9% |

Table 3: Confusion matrices for $E_b/N_0 = -5$ dB.

(a) $n = 1, t = 1$

| | Noise | IEEE 802.16e | IEEE 802.11a |
|---|---|---|---|
| Noise | 99.2% | 0.8% | 0% |
| IEEE 802.16e | 28.1% | 71.7% | 0.2% |
| IEEE 802.11a | 2.8% | 3.6% | 93.6% |

(b) $n = 1, t = 3$

| | Noise | IEEE 802.16e | IEEE 802.11a |
|---|---|---|---|
| Noise | 98.9% | 1.1% | 0% |
| IEEE 802.16e | 13.3% | 86.7% | 0% |
| IEEE 802.11a | 0.2% | 3.3% | 96.5% |

(c) $n = 3, t = 1$

| | Noise | IEEE 802.16e | IEEE |
|---|---|---|---|
| Noise | 99.7% | 0.3% | 0% |
| IEEE 802.16e | 4.1% | 95.8% | 0.1% |
| IEEE 802.11a | 0% | 0.1% | 99.9% |

extracted features (i.e., two real values) have to be exchanged, Adaptive modulation and Coding (AMC) techniques [16] can be used to mitigate this issue. In fact, these techniques enable robust and spectrally-efficient transmission over time-varying channels [16]. In particular, by adding systematically generated redundant data to the exchanged features extracted, it is possible to minimize the channel impairments [16] at the cost of a slight increment of the control channel capacity (i.e., to accommodate redundant data). Note that the smaller the exchanged information the smaller is the quantity of redundant data for minimizing the channel detrimental effects (and then the impact on the control channel capacity). For these reasons, the information reduction phase is proposed for the cooperative single antenna architecture allowing to consider reasonable the assumption of ideal channel.

The increment of the probability of correct detection is more significant for low values of $T_{obs}$ and $E_b/N_0$. In particular, if the cooperative architectures is composed by $n = 3$ CR terminals with $t = 1$ and $E_b/N_0 = -5$ dB, the probability of correct detection increases of 0.1 with respect to the one obtained by the stand-alone single antenna CR terminal (with $n = t = 1$), as shown in Figure 6. A similar behavior is obtained for the multiple antenna architecture, although, in this case, the improvement is less significant for the reasons previously explained. The proposed processing chain for the cooperative and multiple antenna architectures well suited for practical CR networks (e.g., IEEE 802.22 [3]), where CR terminals have to reliably detect the presence of the primary users even in low SNR environment by using a short observation time. In particular, satisfactory correct detection and classification rates are obtained for an observation time of 2 (ms) as reported in Table 2 and in Figure 7. Note that to obtain this results all the considered $E_b/N_0$ are used. Table 2 represents the confusion matrix for the considered classification problem where each value represents the percentage for which the actual signal present (i.e., the rows) is detected and classified as one of the three possible classes of signal (i.e., the columns). The proposed cooperative and multiple antenna architectures show a higher sensitivity than the stand-alone single antenna CR terminal. In fact, the detection rate, reported in Table 2, increases for both architectures for the three considered classes of signal. It is important to note that the main improvement is obtained for the detection of the IEEE 802.16e signal, which is often confused with the noise if a stand-alone single antenna architecture is considered. In fact, these two classes can be confused especially when the received signal is heavily corrupted by channel impairments (see Figure 4), and for this reason spatial diversity of cooperative and multiple antenna systems allows to improve the performance. This is of particular importance in CR networks since when the transmitted signal of the primary user is classified as noise, a false opportunity is detected and consequently a potential harmful interference can arise. The same considerations can be done if an energy per bit to noise power spectral density ratio $E_b/N_0 = -5$ dB, for all the values of $T_{obs}$, is considered, as reported in Table 3.

In order to investigate the capability of the proposed architectures to avoid potential detrimental interference to primary users, the probability of false opportunity detection $P_{fo}$, that is the probability to classify the received signal as noise given the presence of an IEEE 802.16e or an IEEE 802.11a signal, is reported in Figure 8 for the considered $E_b/N_0$ by using all the values of $T_{obs}$. Although here not reported, $P_{fo}$ versus $T_{obs}$ exhibits the same behavior. Note that the probability of false opportunity detection $P_{fo}$ is related to the probability of correct detection $P_{corr}$ as the probability of detection $P_d$ is related to the probability of missed detection $P_{md}$ in classical binary hypothesis testing

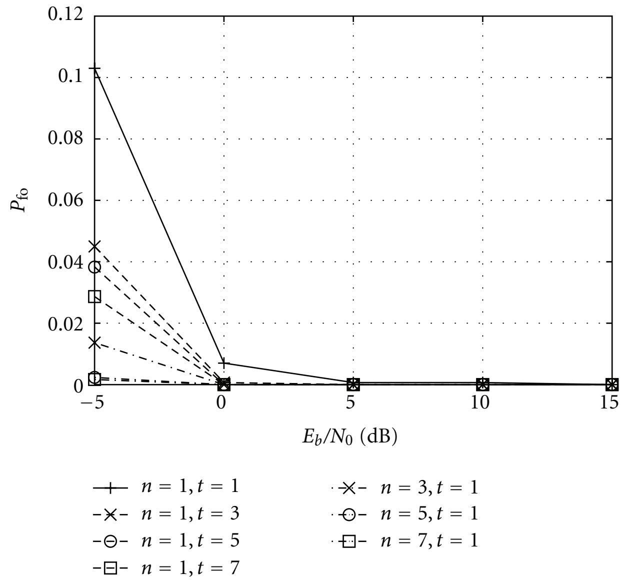


Figure 8: Probability of false opportunity detection $P_{fo}$ versus energy per bit to noise power spectral density ratio $E_b/N_0$ for different numbers $n$ of cooperative single antenna CR terminals and multiple antenna CR terminal with a variable number $t$ of antennas.

Table 4: Comparison of the performances of the proposed architectures.

(a) For $E_b/N_0 = -5$

| Architecture | Parameters | | $P_{corr}$ |
|---|---|---|---|
| Stand-alone single antenna | $n = 1$ | $t = 1$ | 0.8817 |
| Cooperative | $n = 3$ | $t = 1$ | 0.9847 |
| | $n = 5$ | $t = 1$ | 0.9973 |
| | $n = 7$ | $t = 1$ | 0.9983 |
| Multiple antenna | $n = 1$ | $t = 3$ | 0.9403 |
| | $n = 1$ | $t = 5$ | 0.9540 |
| | $n = 1$ | $t = 7$ | 0.9673 |

(b) For $T_{obs} = 2$ ms

| Architecture | Parameters | | $P_{corr}$ |
|---|---|---|---|
| Stand-alone single antenna | $n = 1$ | $t = 1$ | 0.9528 |
| Cooperative | $n = 3$ | $t = 1$ | 0.9928 |
| | $n = 5$ | $t = 1$ | 0.9979 |
| | $n = 7$ | $t = 1$ | 0.9989 |
| Multiple antenna | $n = 1$ | $t = 3$ | 0.9725 |
| | $n = 1$ | $t = 5$ | 0.9776 |
| | $n = 1$ | $t = 7$ | 0.9797 |

problems [19]. In fact, $P_{fo}$ decreases as $P_{corr}$ increases. Moreover, it can be verified graphically from Figures 6 and 8 that $P_{fo} + P_{corr} \approx 1$ (the result is slightly lower than 1 due to those cases where the primary signal is detected but classified into a wrong signal standard, which is not accounted for by $P_{corr}$). In general the performance of the proposed architectures increases as the $E_b/N_0$ and $T_{obs}$ increase, as expected. Moreover, $P_{fo}$ decreases with the number $n$ of cooperative single antenna CR terminals and with the number $t$ of receiving antenna of the multiple antenna CR terminal. As an example, if the multiple antenna system is equipped with $t = 5$ antennas and $E_b/N_0 = -5$ dB, the probability of false opportunity detection decreases of 0.07 with respect to the one obtained by the stand-alone single antenna CR terminal (with $n = t = 1$), as shown in Figure 8. It is important to note that the probability of missed opportunity detection $P_{mo}$, that is, the probability to classify the received signal as an IEEE 802.16e or an IEEE 802.11a signals given the absence of transmission by the primary users, although here not reported, exhibits the same behavior of the presented $P_{fo}$.

Finally, a comparison of the performances of the proposed architectures is presented in Table 4 under specific evaluation conditions, that is, for low values of $E_b/N_0$ and $T_{obs}$. It shows the probability of correct detection $P_{corr}$ for the simulated values $n$ of the cooperative single antenna CR terminals and the number $t$ of the receiving antennas of the multiple antenna CR terminal. Once again it is possible to state that the cooperative and multiple antenna architectures guarantee a significant improvement of the performance with respect to traditional stand-alone single antenna CR terminal, especially under the worst case conditions justifying the extra cost necessary for the implementation of the cooperative single antenna and multiple antenna architectures. For example, for an $E_b/N_0 = -5$ dB (considering all the values of the $T_{obs}$), the cooperative single antenna architecture composed by $n = 3$ terminals allows to increase $P_{corr}$ of about 0.1 with respect to the single antenna architecture.

*6.2. Influence of the Information Reduction Phase on the Performances.* As reported in Section 4.2, an information reduction phase is carried out in order to reduce the amount of data to be processed during the classification phase. On one hand, this reduction enables to shorten the classification time, and hence the entire computational time, allowing to perform opportunity detection and exploitation in real-time. But on the other hand, an incorrect compression can enable a loss in the information used as input to the classifier leading to an undesirable drop of the performances.

In order to evaluate the impact of the information reduction phase in terms of performances and complexity, some numerical results are provided. For the sake of brevity, the obtained performances are reported for the multiple antenna architectures, while some comments are provided for both cooperative single antenna and multiple antenna architectures. In particular, a single multiclass SVM classifier has been designed for each number of receiving antenna by using as input the SCF profile provided by (3) and shown in Figure 4 or the extracted features provided by (4) and shown in Figure 5. Note that the dimension of the input to the multiclass SVM is $(N_{SCF}/\beta) - 1 = 79$ real values in the case of the SCF profile and $i = 2$ real values (i.e., the number of extracted features) in the case of extracted features.

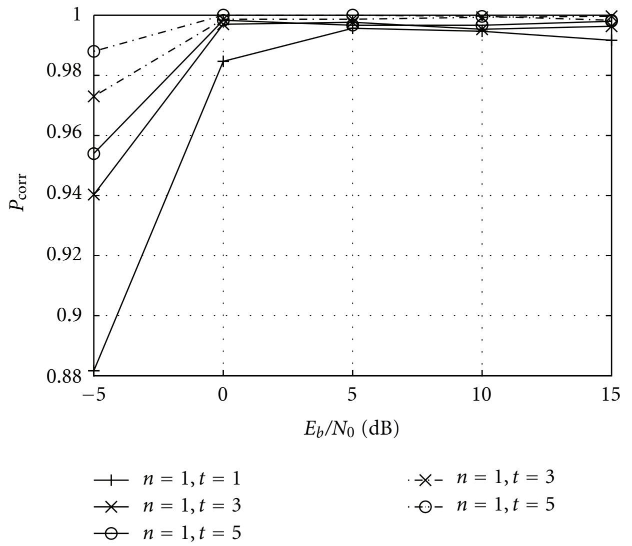


Figure 9: Probability of correct detection $P_{\text{corr}}$ versus energy per bit to noise power spectral density ratio $E_b/N_0$ for different multiple antenna CR terminal with a variable number $t$ of antennas for the extracted features (continuous lines) and for the SCF profile (dotted lines).

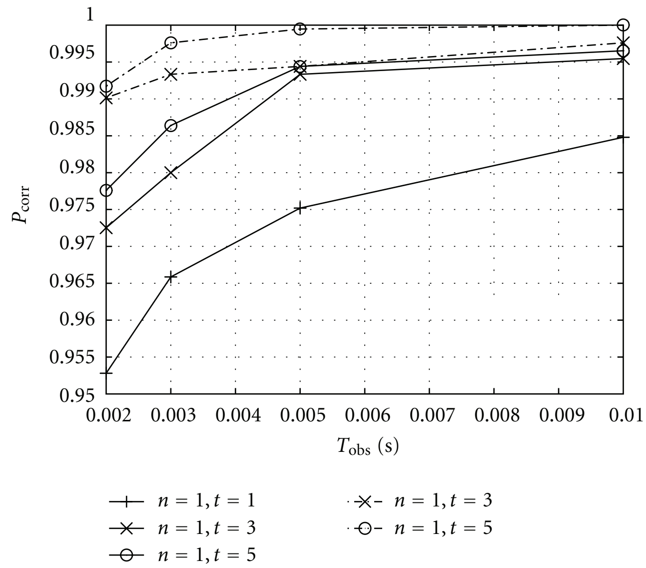


Figure 10: Probability of correct detection $P_{\text{corr}}$ versus observation time $T_{\text{obs}}$ for different multiple antenna CR terminal with a variable number $t$ of antennas for the extracted features (continuous lines) and for the SCF profile (dotted lines).

The probability of correct detection $P_{\text{corr}}$ for the multiple antenna architecture is reported in Figures 9 and 10 for different values of $E_b/N_0$ and $T_{\text{obs}}$, respectively.

It can be deduced that if the SCF profile is used as input to the classification phase then a slight improvement of the performances is obtained with respect to the case in which the extracted features are used. The benefit is greater for low values of $E_b/N_0$ and $T_{\text{obs}}$. As an example, $P_{\text{corr}}$ increases of about 0.03 if the SCF profile is used as input to the classifier and $E_b/N_0 = -5$ dB, for a multiple antenna architecture equipped with 3 or 5 antennas. Note that the same conclusion can be drawn if the cooperative single antenna architecture is considered. However, this improvement is obtained at the cost of an increased elapsed time for the testing phase. Table 5(a) shows the CPU time for testing a single input by using the multiclass SVM classifier for various values of $n$ and $t$. The reported data refers to an Intel Pentium Core 2 CPU working at 1.86 GHz; the code was implemented in C++. It can be deduced that testing an SCF profile requires at least twice the time required to test a set of extracted features for all the considered architectures.

Moreover, if the cooperative single antenna architecture is considered, an increased control channel capacity is required to support the SCF profile exchange. Note that such a channel cannot be available in practical CR scenarios and hence a further information reduction step (i.e., features extraction) could be required. Furthermore, in practical scenarios the exchanged information can be affected by channel impairments which can negatively affect the performances (Table 6). In order to evaluate these effects, it is supposed that the cooperative single antenna terminals share the local extracted features by using a control channel affected by AWGN and multipath distortions (i.e., using the COST 207—Bad Urban channel model, see Table 1). Table 4 shows the performance of a cooperative architecture with different numbers $n$ of single antenna terminals for $T_{\text{obs}} = 3$ ms, using all the considered values of $E_b/N_0$. It can be noted that $P_{\text{corr}}$ decreases as the channel detrimental effects increase, as expected. Although the cooperative architecture shows a satisfactory performance, AMC techniques can be used to mitigate the channel impairments allowing to further improve the performances at the cost of an increased control channel capacity.

Finally, note that for a multiple antenna architecture the information reduction phase is not crucial as for cooperative single antenna architecture. In fact, multiple antenna does not require a dedicated control channel and hence a higher dimension of the input to the classifier can be accepted leading to an improvement of the performances (as shown in Figures 10 and 9). However, this improvement is obtained at the cost of an increased elapsed time for the testing phase which can be undesirable in practical scenarios.

*6.3. Discussion on the Elapsed Time for Processing and Classification Phases.* As far as the computational complexity of the proposed processing chain is concerned, the CPU time for the SCF estimation of the considered signals is reported in Table 5(b), while the CPU time for testing a single input by using the multiclass SVM classifier is reported in Table 5(a) for various values of $n$ and $t$. The reported data refers to an Intel Pentium Core 2 CPU working at 1.86 GHz; the code was implemented in C++.

It is important to note that the elapsed time for SCF estimation increases as $T_{\text{obs}}$ increases, while the elapsed time for testing a single set of features increases as the number $n$ of cooperative CR terminals increases. In fact, the dimension of

Table 5: computational complexity of the proposed processing chain.

(a) Elapsed time for testing a single input

| Architecture | Parameters | | Input type | CPU time (s) |
|---|---|---|---|---|
| Single antenna | $n = 1$ | $t = 1$ | SCF profile | 0.006 |
| | $n = 1$ | $t = 1$ | Extracted features | 0.003 |
| Multiple antenna | $n = 1$ | $t = 3$ | SCF profile | 0.006 |
| | $n = 1$ | $t = 5$ | SCF profile | 0.006 |
| | $n = 1$ | $t = 3$ | Extracted features | 0.003 |
| | $n = 1$ | $t = 5$ | Extracted features | 0.003 |
| Cooperative | $n = 3$ | $t = 1$ | SCF profile | 0.010 |
| | $n = 5$ | $t = 1$ | SCF profile | 0.016 |
| | $n = 3$ | $t = 1$ | Extracted features | 0.004 |
| | $n = 5$ | $t = 1$ | Extracted features | 0.006 |

(b) CPU time for SCF evaluation

| $T_{obs}$ (ms) | CPU time (s) |
|---|---|
| 2 | 0.52 |
| 3 | 0.75 |
| 5 | 1.25 |
| 10 | 2.54 |

Table 6: Effects of channel impairments on the exchanged information.

| Parameters | | Control channel | $P_{corr}$ |
|---|---|---|---|
| $n = 3$ | $t = 1$ | Ideal | 0.9952 |
| $n = 3$ | $t = 1$ | Multipath SNR = 15 dB | 0.9715 |
| $n = 3$ | $t = 1$ | Multipath SNR = 0 dB | 0.9114 |
| $n = 5$ | $t = 1$ | Ideal | 0.9994 |
| $n = 5$ | $t = 1$ | Multipath SNR = 15 dB | 0.9875 |
| $n = 5$ | $t = 1$ | Multipath SNR = 0 dB | 0.9456 |

the set of features $\Upsilon$ increases with $n$, as can be easily deduced from (11).

Despite the fact that the implemented code is not optimized and a general purpose PC has been used for the simulations, the evaluation of the SCF and the testing of a set of features are relatively fast. If a specific purpose processor and optimized code are developed, then even a real-time detection could be possible. Note that the optimization of the code for the SCF estimation is out of scope of the present paper. However, the SCF estimator is based on the DFT. It is well known that this transform can be efficiently implemented by using FFT algorithm allowing to significantly speed up the execution time making it applicable to real-time applications even with traditional hardware [48].

Finally, it is important to note that the elapsed time for processing and classification phases is related to the processing capabilities needed for each considered architecture (see Section 5). In particular, let us suppose that an information reduction step is carried out and the extracted features are used as input to the classification phase. In this case, the processing capabilities at the terminals $P_{\text{terminal}}$ are greater than the ones needed when information reduction is not considered, while the processing capabilities at the fusion center $P_{\text{fusion}}$ decrease since it has to manage the extracted features (i.e., a few bits) instead of a higher amount of information (see Section 4.2). On the contrary, if the information reduction step is not carried out, then the processing capabilities at the terminals $P_{\text{terminal}}$ decrease while the processing capabilities at the fusion center $P_{\text{fusion}}$ increase. As a general consideration, the total amount of the needed processing capabilities $P_{\text{tot}}$ is similar in both cases although distributed in a different way between $P_{\text{terminal}}$ and $P_{\text{fusion}}$. However, if the cooperative architecture is considered, then it is usually preferable to increase $P_{\text{terminal}}$, performing the information reduction step, in order to limit the control channel capacity required.

## 7. Conclusions

In this paper, three architectures, that is, stand-alone single antenna, cooperative and multiple antennas, have been proposed for spectrum sensing. These architectures implement the same advanced signal processing algorithm, based on a cyclostationary analysis which exploits a single SCF estimator and an algorithm to reduce the amount of data given on input to a multiclass SVM classifier for signal detection and classification. Numerical simulations have been carried out in a scenario where primary users can adopt IEEE 802.16e and IEEE 802.11a as transmission standards. This scenario is challenging since both technologies implement a physical layer based on the OFDM technique, with the same bandwidth and frequency band, and the received signals are corrupted by heavy multipath effects. Although the complexity of the considered scenario, the proposed algorithm shows satisfactory performances even if applied to a single antenna terminal architecture. Moreover, the obtained performances can be further improved if the cooperative and the multiple antenna architectures are implemented. In particular, the probability of correct detection increases as the number of cooperative terminals or the number of the receiving antennas of the multiple antenna architecture increase. Moreover, the probability of false opportunity detection and the probability of missed opportunity detection decrease as the number of cooperative terminals and the number of the receiving antennas of the multiple antenna architecture increase. This is of fundamental importance in CR networks where the efficient use of the radio spectrum is the main target. These improvements of the performances are obtained at the price of a rise in hardware costs due to several receiving antennas in the case of multiple antenna architecture or an increment of the overhead due to the presence of a control channel if the cooperative architecture is employed. Finally, it is important to remark that cooperative and multiple antenna architectures allow to shorten the observation time and to improve the overall sensitivity.

## References


[1] S. Haykin, "Cognitive radio: brain-empowered wireless communications," *IEEE Journal on Selected Areas in Communications*, vol. 23, no. 2, pp. 201–220, 2005.

[2] M. Gandetto and C. Regazzoni, "Spectrum sensing: a distributed approach for cognitive terminals," *IEEE Journal on Selected Areas in Communications*, vol. 25, no. 3, Article ID 4155370, pp. 546–557, 2007.

[3] I. F. Akyildiz, W. Y. Lee, M. C. Vuran, and S. Mohanty, "NeXt generation/dynamic spectrum access/cognitive radio wireless networks: a survey," *Computer Networks*, vol. 50, no. 13, pp. 2127–2159, 2006.

[4] B. Farhang-Boroujeny and R. Kempter, "Multicarrier communication techniques for spectrum sensing and communication in cognitive radios," *IEEE Communications Magazine*, vol. 46, no. 4, pp. 80–85, 2008.

[5] T. A. Weiss and F. K. Jondral, "Spectrum pooling: an innovative strategy for the enhancement of spectrum efficiency," *IEEE Communications Magazine*, vol. 42, no. 3, pp. S8–S14, 2004.

[6] T. Yücek and H. Arslan, "A survey of spectrum sensing algorithms for cognitive radio applications," *IEEE Communications Surveys and Tutorials*, vol. 11, no. 1, pp. 116–130, 2009.

[7] W. A. Gardner, "Signal interception: a unifying theoretical framework for feature detection," *IEEE Transactions on Communications*, vol. 36, no. 8, pp. 897–906, 1988.

[8] E. Azzouz and A. Nandi, *Automatic Modulation Recognition of Communication Signals*, Kluwer Academic, Norwell, Mass, USA, 1996.

[9] C. K. Chen and W. A. Gardner, "Signal-selective time-difference of arrival estimation for passive location of man-made signal sources in highly corruptive environments–II: algorithms and performance," *IEEE Transactions on Signal Processing*, vol. 40, no. 5, pp. 1185–1197, 1992.

[10] D. Cabric, S. M. Mishra, and R. W. Brodersen, "Implementation issues in spectrum sensing for cognitive radios," in *Proceedings of the Conference Record of the 38th Asilomar Conference on Signals, Systems and Computers*, pp. 772–776, November 2004.

[11] P. D. Sutton, K. E. Nolan, and L. E. Doyle, "Cyclostationary signatures in practical cognitive radio applications," *IEEE Journal on Selected Areas in Communications*, vol. 26, no. 1, pp. 13–24, 2008.

[12] S. Geirhofer, L. Tong, and B. M. Sadler, "Dynamic spectrum access in the time domain: modeling and exploiting white space," *IEEE Communications Magazine*, vol. 45, no. 5, pp. 66–72, 2007.

[13] R. Chen, J. M. Park, Y. T. Hou, and J. H. Reed, "Toward secure distributed spectrum sensing in cognitive radio networks," *IEEE Communications Magazine*, vol. 46, no. 4, pp. 50–55, 2008.

[14] A. Ghasemi and E. S. Sousa, "Spectrum sensing in cognitive radio networks: requirements, challenges and design trade-offs," *IEEE Communications Magazine*, vol. 46, no. 4, pp. 32–39, 2008.

[15] S. Bellofiore, C. A. Balanis, J. Foutz, and A. S. Spanias, "Smart-antenna systems for mobile communication networks. Part 1: overview and antenna design," *IEEE Antennas and Propagation Magazine*, vol. 44, no. 3, pp. 145–154, 2002.

[16] A. Goldsmith, *Wireless Communications*, Cambridge University Press, Cambridge, UK, 1st edition, 2005.

[17] T. S. Rappaport, *Wireless Communications: principles and Practice*, Prentice Hall, New York, NY, USA, 2nd edition, 2002.

[18] W. C. Y. Lee, *Mobile Communications Engineering: Theory and Applications*, McGraw-Hill, New York, NY, USA, 2nd edition, 1997.

[19] P. K. Varshney, *Distributed Detection and Data Fusion*, Springer, New York, NY, USA, 1st edition, 1996.

[20] H. Urkowitz, "Energy Detection of unknown deterministic signals," *Proceedings of IEEE*, vol. 55, pp. 523–531, 1967.

[21] L. Bixio, M. Ottonello, M. Raffetto, and C. S. Regazzoni, "Performance evaluation of a multiple antenna system for spectrum sensing," in *Proceedings of the IEEE International Symposium on Antennas and Propagation*, North Charleston, SC, USA, June 2009.

[22] R. Hachemani, J. Palicot, and C. Moy, "A new standard recognition sensor for cognitive terminal," in *Proceeding of the European Signal Processing Conference*, 2007.

[23] K. Ahmad, U. Meier, and H. Kwasnicka, "Fuzzy logic based signal classification with cognitive radios for standard wireless technologies," in *Proceedings of the 5th International Conference on Cognitive Radio Oriented Wireless Networks and Communications (CROWNCom '10)*, pp. 1–5, Cannes, France, June 2010.

[24] V. Chen and H. Ling, "Joint time-frequency analysis," *IEEE Signal Processing Magazine*, vol. 16, no. 2, pp. 52–67, 1999.

[25] M. Öner and F. Jondral, "On the extraction of the channel allocation information in spectrum pooling systems," *IEEE Journal on Selected Areas in Communications*, vol. 25, no. 3, pp. 558–565, 2007.

[26] A. Fehske, J. Gaeddert, and J. H. Reed, "A new approach to signal classification using spectral correlation and neural networks," in *Proceedings of the 1st IEEE International Symposium on New Frontiers in Dynamic Spectrum Access Networks (DySPAN '05)*, pp. 144–150, Baltimore, Md, USA, November 2005.

[27] K. Kim, I. A. Akbar, K. K. Bae, J. -S. Um, C. M. Spooner, and J. H. Reed, "Cyclostationary approaches to signal detection and classification in cognitive radio," in *Proceedings of the 2nd IEEE International Symposium on New Frontiers in Dynamic Spectrum Access Networks*, pp. 212–215, Dublin, Ireland, April 2007.

[28] L. Bixio, A. F. Cattoni, C. S. Regazzoni, and P. K. Varshney, "Autonomic computing and networking," in *Embodied Cognition-Based Distributed Spectrum Sensing for Autonomic Wireless Systems*, Springer, New York, NY, USA, 2009.

[29] B. A. Fette, *Cognitive Radio Technology*, Newnes, Oxford, UK, 2006.

[30] A. K. Jain, R. P. W. Duin, and J. Mao, "Statistical pattern recognition: a review," *IEEE Transactions on Pattern Analysis and Machine Intelligence*, vol. 22, no. 1, pp. 4–37, 2000.

[31] R. P. Lippmann, "Pattern classification using neural networks," *IEEE Communications Magazine*, vol. 27, no. 11, pp. 47–59, 1989.

[32] B. Ramkumar, "Automatic modulation classification for cognitive radios using cyclic feature detection," *IEEE Circuits and Systems Magazine*, vol. 9, no. 2, pp. 27–45, 2009.

[33] L. Bixio, G. Oliveri, M. Ottonello, and C. S. Regazzoni, "OFDM recognition based on cyclostationary analysis in an open spectrum scenario," in *Proceeings of the IEEE 69th Vehicular Technology Conference (VTC '09)*, Barcelona, Spain, April 2009.

[34] V. Kecman, *Learning and Soft Computing: Support Vector Machines, Neural Networks, and Fuzzy Logic Models*, MIT Press, Cambridge, Mass, USA, 2001.

[35] S. Gunn, "Support vector machine for classification and regression," Tech. Rep., University of Southampton, Southampton, UK, 1988.

[36] C.-C. Chang and C.-J. Lin, "LIBSVM: a library for support vector machines," 2001, http://www.csie.ntu.edu.tw/~cjlin/libsvm/.

[37] C. W. Hsu, C. C. Chang, and C. J. Lin, "A practical guide to support vector classification," Tech. Rep. 106, Department Of Computer Science National Taiwan University, Taipei, Taiwan, 2008.

[38] C. Bishop, *Pattern Recognition and Machine Learning*, Springer, New York, NY, USA, 2006.

[39] L. Bixio, G. Oliveri, M. Ottonello, M. Raffetto, and C. S. Regazzoni, "Cognitive radios with multiple antennas exploiting spatial opportunities," *IEEE Transactions on Signal Processing*, vol. 58, no. 8, pp. 4453–4459, 2010.

[40] L. Bixio, M. Ottonello, M. Raffetto, C. S. Regazzoni, and C. Armani, "A comparison among cooperative spectrum sensing approaches for cognitive radios," in *Proceedings of the 2nd International Workshop on Cognitive Information Processing (CIP '10)*, pp. 168–173, Elba Island, Italy, June 2010.

[41] L. Bixio, M. Ottonello, H. Sallam, M. Raffetto, and C. S. Regazzoni, "Signal classification based on spectral redundancy and neural network ensembles," in *Proceedings of the 4th International Conference on Cognitive Radio Oriented Wireless Networks and Communications (CROWNCOM '09)*, Hannover, Germany, June 2009.

[42] L. Bixio, M. Ottonello, M. Raffetto, and C. S. Regazzoni, "A comparison between stand-alone and distributed architectures for spectrum hole detection," in *Proceedings of the IEEE Wireless Communications and Networking Conference (WCNC '10)*, April 2010.

[43] H. Ishii and G. W. Wornell, "OFDM blind parameter identification in cognitive radios," in *Proceedings of the IEEE 16th International Symposium on Personal, Indoor and Mobile Radio Communications (PIMRC '05)*, pp. 700–705, September 2005.

[44] IEEE 802.16-2005, "IEEE standard for local and metropolitan Area Network Part 16: Air Interface for Fixed Broadband Wireless Access System Amendament 2: Physical and Medium Access Control Layer for Combined Fixed and Mobile Operations in Licensed Bands," December 2005.

[45] IEEE 802.11-1999, "IEEE standard for local and metropolitan Area Network Part 11: Wireless LAN Medium Access Control (MAC) andPhysical Layer (PHY) specifications High-speed Physical Layer in the 5 GHz Band," 1999.

[46] M. Patzold, *Mobile Fading Channels*, John Wiley & Sons, New York, NY, USA, 2002.

[47] M. Gandetto, M. Guainazzo, and C. S. Regazzoni, "Use of time-frequency analysis and neural networks for mode identification in a wireless software-defined radio approach," *Eurasip Journal on Applied Signal Processing*, vol. 2004, no. 12, pp. 1778–1790, 2004.

[48] X. -F. Li, C. Long, and W. Shihu, "The implementation of high-speed FFT processor based on FPGA," in *Proceedings of the International Conference on Computer, Mechatronics, Control and Electronic Engineering (CMCE '10)*, vol. 2, pp. 236–239, Changchun, China, August 2010.